Bistability in bubble formation

Eduardo Colli*
Instituto de Matemática e Estatística, Universidade de São Paulo, R. do Matão 1010, CEP 05508-090 São Paulo, Brazil

Viviane S. M. Piassi, Alberto Tufaile, and José Carlos Sartorelli†
Instituto de Física, Universidade de São Paulo, Caixa Postal 66318, 05315-970 São Paulo, Brazil
(Received 23 July 2004; published 23 December 2004)

We obtain experimental data on time intervals of a bubble train generated from a nozzle with the air flow rate as the control parameter. Varying the length of the hose that connects the proportionating solenoid valve to the nozzle, we generate bifurcation diagrams showing period-adding cascades, among other dynamical phenomena. Then we construct a two-parameter family of one-dimensional maps whose bifurcation diagrams qualitatively match the experimental ones. The model indicates the existence of parameters where two attractors coexist, a phenomenon called bistability, and the same behavior is fully confirmed in the experiment.

DOI: 10.1103/PhysRevE.70.066215 PACS number(s): 05.45.−a, 47.55.Dz, 47.52.+j

I. INTRODUCTION

Bubble formation in a nozzle is a common phenomenon that can be observed in everyday situations, from aquarium to champagne glasses [1]. The shape of bubbles and the interaction between them are the center of interest for many interfacial studies and technological processes from petrochemical to food industries [2] and space crafts [3]. Nevertheless, bubble formation has only really begun to be properly explored in the last few decades due to the development of experimental and computational techniques, which gave access to completely new phenomena. Besides these developments, the introduction of nonlinear dynamics has thrown some light on the understanding of transitions between different bubbling regimes, enabling the recognition of periodic and chaotic behavior. Considering a bubble as an object resulting from the interplay between a pneumatic and a liquid system, the bubble formation depends on the many elements such as geometrical and physical-chemical parameters. In this direction some attempts have been made to introduce models which could mimic some of the properties of bubble formation and provide a path to their understanding [4,5].

Our emphasis in this paper resides on time scale quantities of a bubble train generated in a nozzle at different air flow rates. More precisely, we look at the time series of time intervals T_n between successive bubbles and investigate the correlation between two successive time intervals. Experimental results [5–8] have shown that the sequence $\{T_n\}$ is not necessarily constant. Stable periodic regimes of period greater than one or even chaotic regimes may appear. In fact, it is demonstrated that this sequence is approximately given by the iterates of a one-dimensional map, that is, $T_{n+1} = f(T_n)$. In this work we propose a more accurate model that generates this map. Both in the experiment and in the model the dynamics is investigated through a bifurcation diagram which is the plotting of the attracting sets against a control parameter, which in the experimental case is the air flow rate. Some interesting features such as *period-adding cascades* appear in these diagrams [5], a phenomenon already reported in different contexts, such as firing neurons [9,10], electric circuits [11], and pulsing lasers [12].

Another important aspect is *bistability*, which is the coexistence of two stable periodic regimes for the same control parameter. Bistability arises naturally in theoretical models showing period-adding cascades and is fully confirmed in our experiments. This phenomenon implies a shift in the bifurcation parameters, according to how the experiment is conducted, that seems at first sight to be an experimental error [13], but in fact is intrinsic to the dynamics and can be explained by theory.

This paper is organized as follows. In Sec. II we describe the experimental apparatus. In Sec. III we present a comparison between the experimental bifurcation diagrams and those obtained numerically from the model, explaining then both the physical and phenomenological motivations of its construction. In Sec. IV we study the essential mechanisms of period-adding bifurcations and in Sec. V we obtain confirmation, from the experimental point of view, of the predicted phenomenon of bistability.

II. EXPERIMENTAL APPARATUS

The bubble column consists of a cylindrical tube with an inner diameter of 11 cm and 70 cm in height. The bubbles are issued by injecting air through a metallic nozzle submerged in a viscous fluid (20% water/80% glycerol) and the liquid is maintained at a level of 15 cm, as shown in Fig. 1. The nozzle with inner diameter of 0.78 mm and length of 2.5 cm is placed with its tip 6.5 cm below the liquid surface to avoid wall effects on the forming bubble. The nozzle is attached to a chamber with a capacity of 30 ml. Air from a compressor is injected to a capacitive reservoir and a proportionating solenoid valve (Aalborg PSV-5) controlled by a PID controller (BTC-220) sets the air flow to the chamber under the nozzle. The flow rate is measured by a flow-meter (Aalborg GFM47). The pressure drop across the solenoid

*Electronic address: colli@ime.usp.br
†URL: http://www.fge.if.usp.br/~sartorel/lab.html

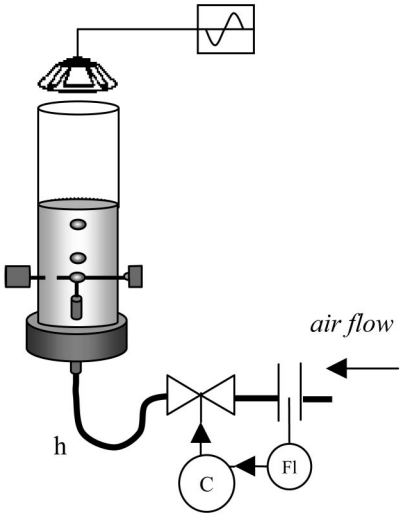

FIG. 1. Experimental apparatus for bubble formation with the flowmeter (Fl), the controller (C) and the solenoid valve, representing the control loop of the air flow rate, and the hose (h) between the valve and the chamber under the nozzle.

valve is around 50 kPa for the working range of air flow rate.

In order to study the influence of the pneumatic system in the bubble formation dynamics, a hose is connected from the solenoid valve to the chamber under the nozzle, keeping fixed the influence of the other elements of the pneumatic system. The hose inner diameter is 4.1 mm and we used four different hose lengths: 10.0 cm, 50.0 cm, 135.0 cm, and 307.0 cm. The hose lengths change intrinsic properties of the pneumatic system, such as the inertance, which represents the phase difference between pressure and mass flow. The hose volumes are 1.3, 6.6, 17.8, and 40.5 ml, which gives an idea of the relative volumes of the bottom chamber and the air line.

Using a ramp function of the controller, the air flow rate ranged from 65 to 125 ml/min. We also perturbed the bubble formation dynamics applying sound bursts with a loud speaker placed near the top of the bubble column.

The detection system is based on a laser-photodiode with a horizontal He-Ne laser beam focused in photodiode placed 2 mm above the nozzle. The time interval between successive bubbles is measured by the time circuitry inserted in a PC slot with a time resolution equal to 1 μs. The input signals are voltage pulses induced in a resistor and defined by the beginning (ending) of scattering of a laser beam. The pulse width is the time interval t_n (n is the bubble number) and the time delay between two pulses defines the crossing time (dt_n) of a bubble through the laser beam, so that the total time interval is $T_n = t_n + dt_n$. We estimate the total experimental noise around 100 μs in the period 1 behavior; see [6] for more details.

III. BIFURCATION DIAGRAMS

The experimental results are summarized in the four bifurcation diagrams shown in Figs. 2(a)–2(d), corresponding to the four hoses in increasing order of length.

The time interval between bubbles (vertical axis) was recorded while slowly increasing the air injection rate (horizontal axis) into liquid. For the shortest hose (10.0 cm)—Fig. 2(a)—the bubbling dynamics is a period 1 regime for this range of flow rate. In Fig. 2(b) the effect of hose lengthening (50.0 cm) is shown by a closed looplike sequence called *bifurcation bubble* around 115 ml/min. The stable period 1 regime gives rise to a stable period 2 regime (a period-doubling bifurcation) and then reverses to a period 1 regime again (a reverse period-doubling bifurcation or period-halving bifurcation). Figure 2(c) shows the bifurcation sequence for the hose length of 135.0 cm presenting a more complex scenario, including period 3 and chaos. Finally, in Fig. 2(d), using the longest hose, we see the period-adding cascade, where successive stable periodic regimes of increasing period appear as the air flow rate increases. The cascade is sudden interrupted by the appearance of a period 1 stable regime.

These experimental bifurcation diagrams were emulated by the following model:

$$f_{l,\phi}(T) = -\phi + \{\text{greatest root of } t \mapsto T + m[t - d(T)]^3 - l[t - d(T)]\}, \quad (1)$$

where $d(T) = -A[1 - \tanh(T + B)]$ and $m = 0.4$, $A = 2.4$, and $B = 1.4$ are fixed parameters. In this model, T is the time interval between bubbles, the control parameter ϕ plays the role of the air flow rate in the diagrams and the parameter l plays the role of the hose length. Figures 2(A)–2(D) show the numerical experiments with four different values of l, say −1.0, −0.55, 0.0, and +1.2, respectively. We have chosen the values of l generating the best possible qualitative emulations of the real bifurcation sequences. The inspiration to our model comes from three sources.

(1) Glimpses of the shape of f coming from the diagram T_{n+1} vs T_n for parameters with chaotic dynamics. In this case there are many different pairs $(T_n, T_{n+1}) = [T_n, f(T_n)]$ giving a rough idea of at least a region of the graph.

(2) Glimpses of the shape of f by the properties of its dynamics: the bubble bifurcation for the small hose and the period-adding cascade for long hoses.

(3) Examination of "greatest root models" that may generate discontinuities.

Two examples of (1) are shown in Fig. 3, for hose lengths equal to 130.0 cm and 140.0 cm and air flow rate around 105 ml/min. In Fig. 3(a) the plot suggests a continuous function with an inflection point in the decreasing branch and in Fig. 3(b) a discontinuity point near the same region. For nonchaotic dynamics our assumption is that the main features of the graph are preserved and its shape is continuously deformed as the parameters change.

Another less canonical method is to obtain transient iterates outside equilibrium by perturbing and relaxing the system (with a sound burst, for example). The problem with this method is that the perturbation changes the system itself, that is, exactly the function f we want to determine. In fact, one has to observe the transient regime immediately after removing the sound, but it is never sure that the system has returned to its unperturbed condition before these iterates. It is

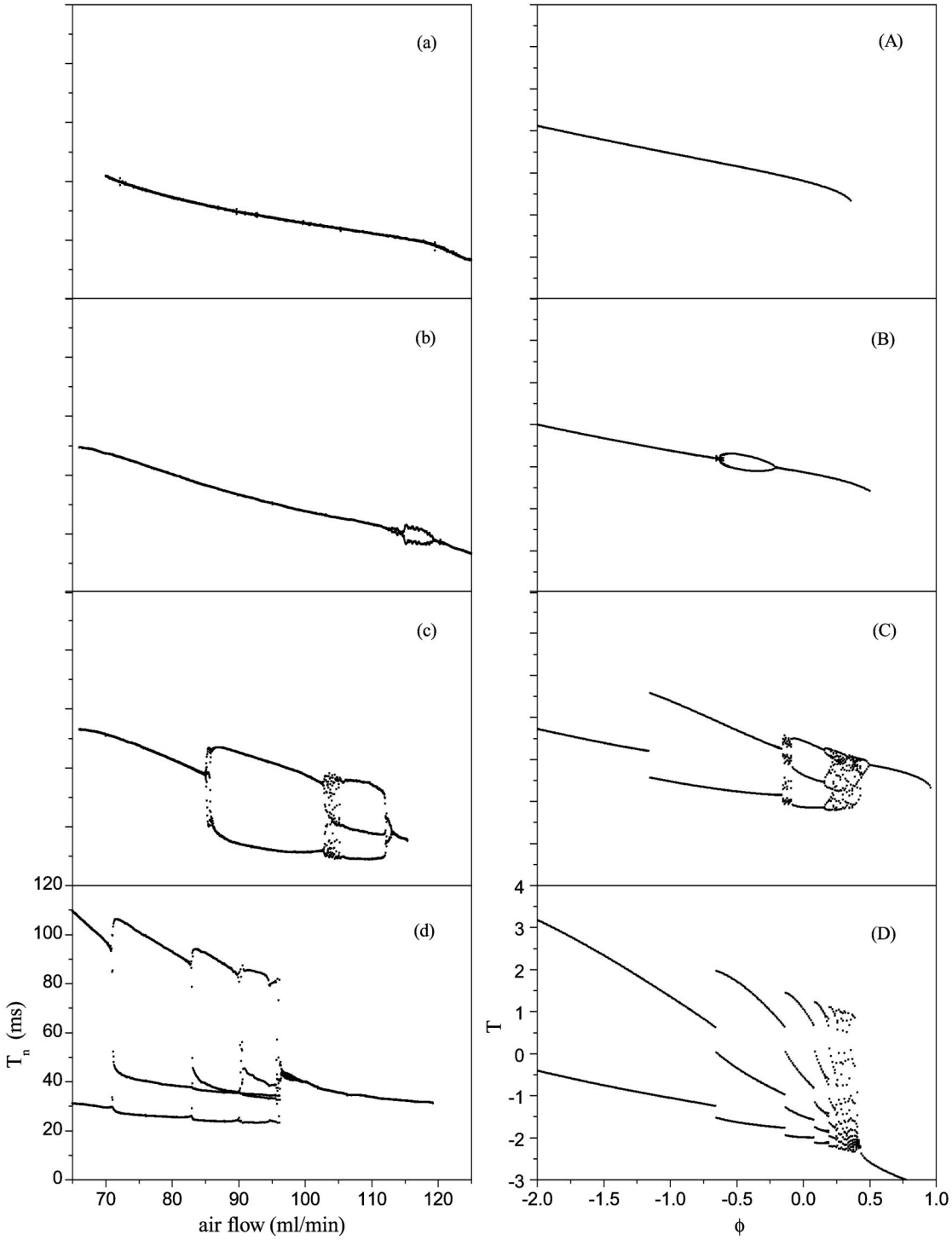

FIG. 2. (a)–(d) Bifurcation diagrams produced by the experiment with hose lengths 10.0 cm, 50.0 cm, 135.0 cm, and 307.0 cm, respectively. (A)–(D) Bifurcation diagrams produced by a computer experiment with model (1), with parameter l equal to −1.0, −0.55, 0.0, and +1.2, respectively.

pratically impossible to push the bubbles to a transient regime without affecting the system we want to observe.

However combining the positive aspects coming from (2) and (3) we were able to fulfill these lacks of information.

Concerning (2), if the dynamics is periodic little can be said about the shape of f, but the variation of a parameter induces a movement in the graph that has consequences on the bifurcation diagram. For example, for long hoses the period-adding cascade suggests a mechanism of increasing period and a discontinuity of f (as we will see later in Sec. IV). For short hoses, the bubble bifurcation suggests a decreasing branch of f with an inflection point. For if (a) the derivative is greater than one in absolute value at the inflection point, (b) the derivative is smaller than one a bit farther

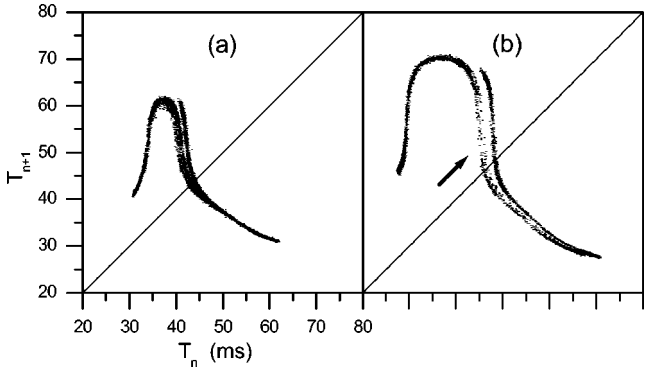

FIG. 3. Two examples of chaotic dynamics in the diagram T_{n+1} vs T_n. (a) Hose length of 130.0 cm. The plot suggests a continuous function with an inflection point in the decreasing branch. (b) Hose length of 140.0 cm. Here the plot suggests a discontinuity in the decreasing branch, indicated by the arrow.

from the inflection point and (c) the graph moves with respect to the diagonal with the variation of the control parameter, then the fixed point given by the intersection between the graph and the diagonal may lose and recover its stability by period-doubling and period-halving bifurcations.

All these considerations show that the hose length affects the shape of f more or less as depicted in Fig. 4. As long as the hose length increases the smooth inflection becomes stronger, giving rise to a discontinuity.

A discontinuity like this can be generated by a greatest root model. For each T we associate a function $F_T(t)$ and determine $f(T)$ as its greatest root. A discontinuity in the function f may appear if F_T is not monotone. If F_T changes more or less as in Fig. 5, for example, for increasing T, then there is a jump in the value of $f(T)$ exactly for the parameter T such that the critical value touches the abscissa.

The function $F_T(t)$ was chosen to be always a cubic in the variable t. The starting point was the function mt^3-lt, where l plays the role of the hose length. Note that for negative values of l this function has no critical points, and for positive values it has two. Hence it is exactly for positive values of l that a discontinuity in f appears. The graph of $F_T(t)=T+m[t-d(T)]^3-l[t-d(T)]$ is the graph of mt^3-lt displaced by T in the vertical direction and by $d(T)$ in the horizontal direction. The choice of $d(T)$ is done in such a way that this displacement is almost null for positive T (approximately corresponding to the right side of the discontinuity) and decreases to a negative asymptotic value for negative T, forcing f to resemble the experimental data, more or less as depicted

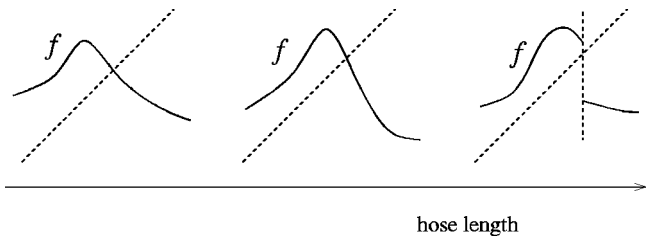

FIG. 4. Depiction of the evolution of f with increasing hose length. The inflection point gives rise to a discontinuity.

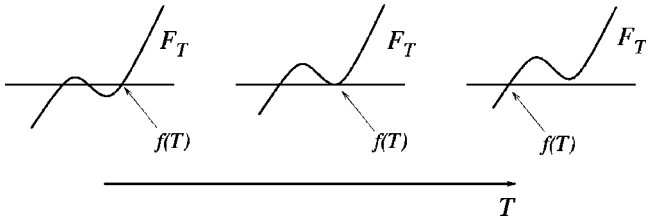

FIG. 5. A family of functions F_T that produces a discontinuity in the greatest root.

in Fig. 4. The parameter ϕ, which plays the role of the air flow rate, shifts the graph of f in the vertical direction.

Although the essential features of bubbling dynamics are dominated by the unimensional model, a more accurated reproduction of the data shown in Fig. 3 requires an extra dimension in the model. This can be done for supposing that the time interval between two bubbles depends on the two previous time intervals, instead of just the last one, such as

$$T_{n+1} = f_{l,\phi}(T_n) + bT_{n-1},$$

which adds a term that depends linearly on the penultimate time interval. Although Fig. 6 shows two plots T_{n+1} vs T_n of this dynamics that could be compared with the diagrams of Fig. 3, this additional term gives no important qualitative contribution for relatively small b, justifying the use of unidimensional maps.

IV. PERIOD-ADDING CASCADES

The main ingredient of period-adding cascades in one-dimensional families of maps is *discontinuity*. The subject is not new [14–16], but here the aim is at giving a qualitative description of the phenomenon directly in model (1). As a consequence, this led us to predict the occurrence of *bistability* in the experiment, as explained in Sec. V.

In this analysis ϕ is the control parameter and the others must remain fixed. The parameter l is suitably chosen in order that $f=f_{l,\phi}$ show a discontinuity; see Fig. 7. The understanding of the dynamics comes from the study of the *first return map* of iterates of f departing from the region to the right of the discontinuity, as illustrated in Fig. 7 with a typical trajectory.

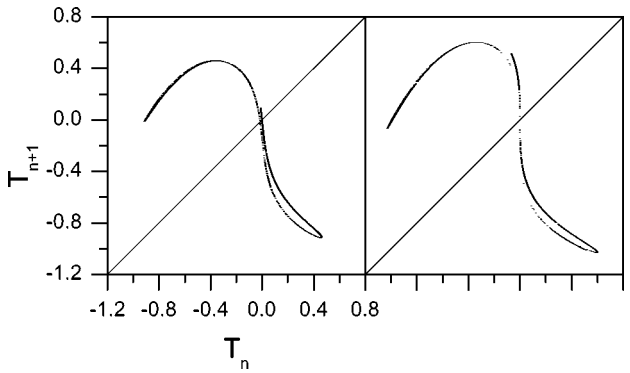

FIG. 6. Two examples of chaotic dynamics in the diagram T_{n+1} vs T_n for the adapted model $T_{n+1}=f(T_n)+bT_{n-1}$. (a) $l=-0.1$, $\phi=-0.12$, and $b=-0.15$. (b) $l=0.0$, $\phi=-0.172$, and $b=-0.1$.

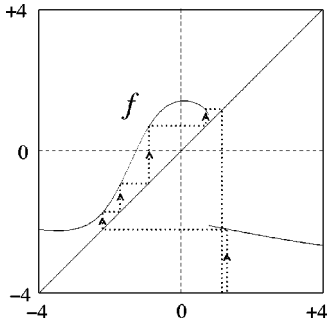

FIG. 7. Graph of model (1) for $l=1.2$ and $\phi=0.03$. The dotted path indicates the iterates of a starting condition until the first return to the right of the discontinuity.

A key element determining the number of iterates for returning is the proximity between the diagonal and the left branch of f. This proximity is controlled by the parameter ϕ, which moves the graph in the vertical direction. As ϕ approaches the value ϕ^* for which a saddle-node bifurcation appears the number of iterates for returning increases to infinity.

The first return map to an interval I, under f, is the map which associates to each T in I the point $f^k(T)$, where $k=k(T)$ is the first positive integer such that $f^k(T)$ belongs to I, which will be called the *return iterate* of T. Note that in general it is not true that the return map is defined for all points in I, since there may be points whose future orbits never return. But this is not a serious problem in our setting, since as long as the left branch of f remains above the diagonal there will be always a return iterate, except for one orbit that lands exactly on the discontinuity (where f is not defined).

The choice of the interval I in model (1) is done in the natural way. The *left boundary point of I is defined as the discontinuity point*, which can be explicitly calculated and is equal to $2m(l/3m)^{3/2}$. Its location is independent of the parameter ϕ. The *right boundary point of I is defined as the critical value*, which is the maximum attained by f in the region into consideration. Calling x_c the critical point, which is independent of ϕ, the critical value is given by $f_{l,0}(x_c)-\phi$. The point x_c may be numerically evaluated by finding the intersection between the solution of $(\partial G/\partial T)=0$, where $G(t,T)=T+m[t-d(T)]^3-l[t-d(T)]$, with the graph of $f_{l,0}$. We found $f_{l,0}(x_c)=1.461246\ldots$ in this way.

Once chosen the interval $I=I(\phi)$, one may regard the evolution of its first return map with the parameter ϕ. For example, Fig. 8 shows a sequence of snapshots of the first return map for increasing parameter values. At $\phi=0.00$ the return map is a single branch crossing the diagonal with negative slope and derivative smaller than one in absolute value. This implies that there is an attracting fixed point (for the return map) in I, and it turns out that this point attracts every orbit starting in I. Moreover, the conclusion may be extended to f, as the return map is simply the 4th iterate of f: the attracting fixed point of f^4 is one point of an attracting 4-cycle of f.

For $\phi=0.02$ and $\phi=0.04$, in the same figure, the return map has also a 5-branch, but the asymptotic behavior of

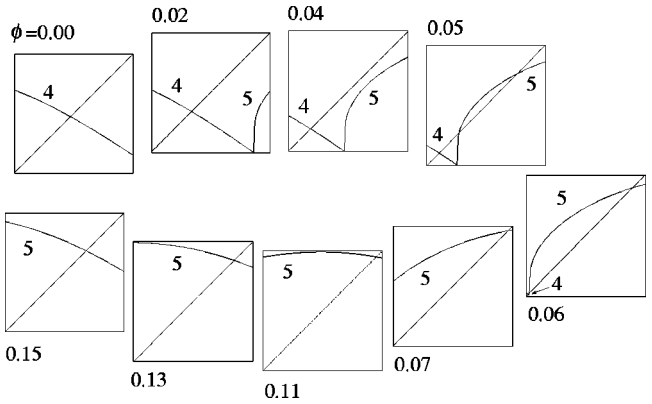

FIG. 8. Evolution of the return function with ϕ for $l=1.2$. Numbers 4 and 5 indicate the iterate of $f_{l,\phi}$. Note that in this sequence the 4-branch has an attracting fixed point. The 5-branch evolves in the following way: it starts with no fixed point, then it creates two fixed points, one attracting and the other repelling, and finally the repelling fixed point disappears, letting this branch in the same situation as the 4-branch was at the beginning.

orbits is the same as the one described above for $\phi=0.00$. The significant change occurs when the 5-branch touches the diagonal, creating an extra pair of fixed points, one attracting and the other repelling. Now the two attracting fixed points are alternatives for the asymptotic limit of the orbits and, except for the repelling fixed point, every orbit goes to one or to the other. For the original map f, this implies the existence of two attracting cycles, of periods 4 and 5.

For $\phi=0.07$ it only remains the attracting fixed point of the 5-branch, and this is still true for parameters a bit beyond $\phi=0.15$. For higher values of the parameter the return map experiences the same transformations, the 5-branch sharing space with the 6-branch and then disappearing, letting the 6-branch alone, and so on. At the same time, the bifurcation diagram shows a single attracting cycle of period 5, then attracting 5 and 6 cycles coexisting, then a single attracting cycle of period 6, and so on. This fully explains the period-adding cascades shown in the diagrams.

The reasoning above shows that in the transition regions of the parameter where period increases by one unit two attractors coexist, a phenomenon called *bistability*. We address this matter in the next section, mainly concerning its consequences to the experimental data.

V. BISTABILITY

The most striking feature of this experiment is the phenomenon of bistability, which becomes clear in view of the theoretical explanation of what is a period-adding cascade; see Sec. IV. However, it is not so easy to detect bistability merely by the experiment and the reason resides in the way a bifurcation diagram is obtained.

When drawing a bifurcation diagram by a computer experiment one often proceeds in the following way. The parameter (which is ϕ, in our case) is allowed to vary within a certain range. For each parameter, a starting condition is chosen, iterations are done, the first of them are thrown away

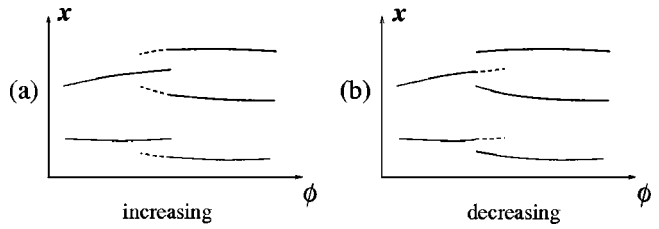

FIG. 9. Drawing of what bifurcation diagrams may show in a computer experiment where the initial condition for each parameter is chosen as the last iterate of the previous parameter. Full lines indicate what is plotted in the diagram and dashed lines the attractor that coexists but does not appear. (a) Increasing values of the parameter; (b) decreasing values of the parameter. If the diagrams are compared, the transition from one regime to another happens in different places.

and a certain number of them are plotted with abscissa equal to the parameter and ordinate equal to their values. But if for each parameter only one starting condition is chosen then as a result only one attractor for that parameter will be seen. Although good for systems with just one attractor (the quadratic family, for example), this method fails in general.

There are two classical ways of choosing a starting condition for each parameter. One is simply by fixing a value that will be used for all parameters. The other is to assume the starting condition to be the last iteration done for the previous parameter. The former method is somewhat arbitrary and has no connection with the dynamics. In the latter case, if an attractor persists from one parameter to the other then the starting condition will be already very near the attractor and there will be almost no chance of converging to the other attractor. Thus, if the attractor appearing in the bifurcation diagram ceases to appear from one parameter to the next then it is possible to conclude that it has no continuation at all.

The schematic drawing of Fig. 9(a) shows what happens in a transition of a period-adding cascade when the parameter is varied from the left to the right and the starting condition is taken as the last iterate of the previous parameter. Full lines show what we would see in the plotted diagram, although dashed lines indicate that another attractor does exist. However, our vision would be different if the parameter was allowed to decrease, as shown in Fig. 9(b), things working like a hysteresis.

The bifurcation diagrams drawn by the experiment work more or less in the same way. With the aid of the ramp, the air flow rate is slowly varied and the time intervals between bubbles are recorded. The only difference is that the parameter is continuously changed and, at least theoretically, a bubble is formed with a different parameter from that of the previous one. However, if the ramp is sufficiently slow this will be of no practical importance. In fact, this is the best way of producing bifurcation diagrams.

Figures 10(a) and 10(b) show two experimental bifurcation diagrams exhibiting a period-adding cascade, one for an increasing and the other for a decreasing ramp, the remaining parameters kept fixed. The shift in the parameter values for which period changes occur is not due to experimental errors or uncontrollable variables but is fully confirmed by the theoretical remarks above. In Figs. 10(A) and 10(B) the same experiment is done with model (1) and the result is very similar.

Bistability can also be directly accessed by the following experiment. Fix an air flow rate corresponding to a transition window where two periodic attractors coexist. The system will stabilize in one of the periodic regimes. Now with a sound burst perturb and relax the system in order that a transient regime appears. If the perturbation is sufficiently strong it can move the transient orbit to the basin of the other attractor. Figure 11 shows the time series for a fixed value of the air flow rate in a transition window between periods 2

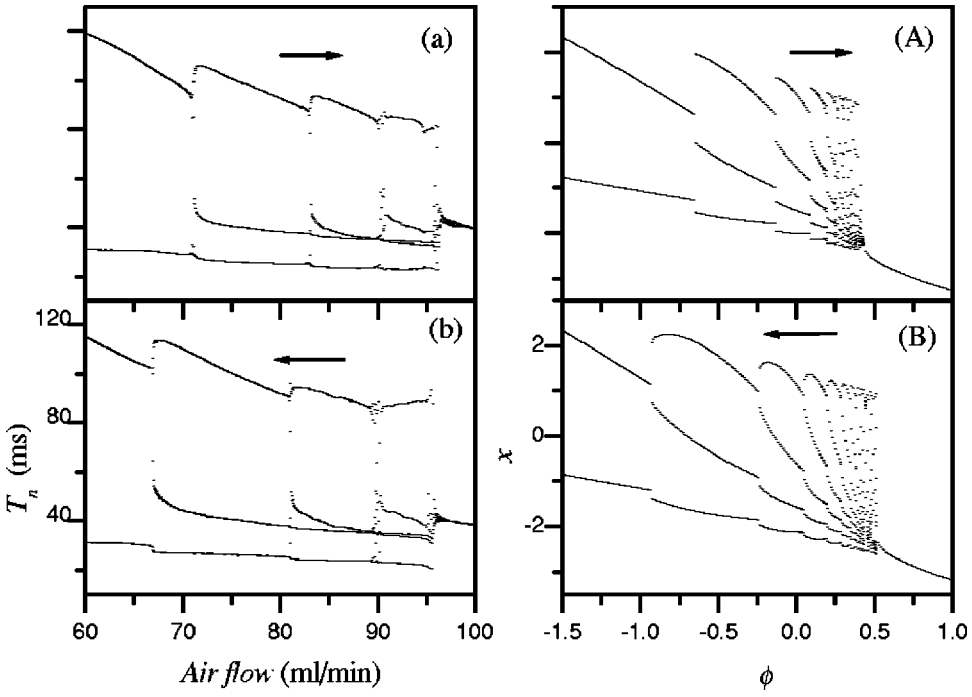

FIG. 10. (a),(b) Experimental bifurcation diagrams with increasing and decreasing ramps, for the longest hose length. (A),(B) Computer generated bifurcation diagrams from model (1) with increasing and decreasing parameters, always taking as initial condition the last iterate of the previous parameter.

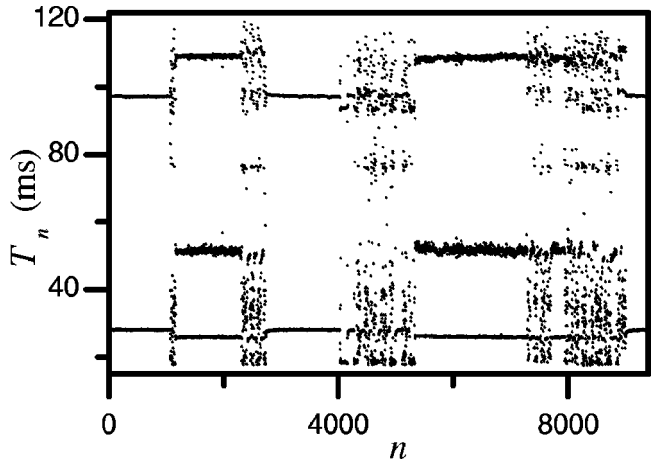

FIG. 11. Time series indicating the coexistence of two different periodic bubbling regimes with a period two and a period three. It is possible to switch between the attractors using sound bursts. The air flow rate was kept constant at 69.7 ml/min.

and 3, with a sequence of sound bursts revealing two coexisting stable regimes. Finally, Fig. 12 shows the bubbling profiles for these two stable period bubbling regimes.

VI. CONCLUSIONS

We obtained experimental data on time intervals of a bubble train generated from a nozzle at different air flow rates. The bifurcation diagrams showed bubble bifurcations (a period-doubling followed by a period-halving bifurcation) and period-adding cascades, accordingly to the length of the hose connecting the flow controller to the chamber under the nozzle. These diagrams were successfully reproduced by a two-parameter family of maps constructed with a greatest root model, one parameter (ϕ) qualitatively playing the role of the air flow rate and the other (l) of the hose length. These maps have a point of discontinuity for $l>0$ which is associated to the period-adding cascades. For $l<0$ there is only an inflection point with derivative going to infinity as l goes to zero. This inflection point explains the bubble bifurcations (period-doubling followed by period-halving) for a short hose.

With this model we better understood the apparent inconsistencies between diagrams obtained with increasing and decreasing ramps. They are explained by the phenomenon of bistability that occurs in the transition between periods in a period-adding cascade and the way a bifurcation diagram is drawn.

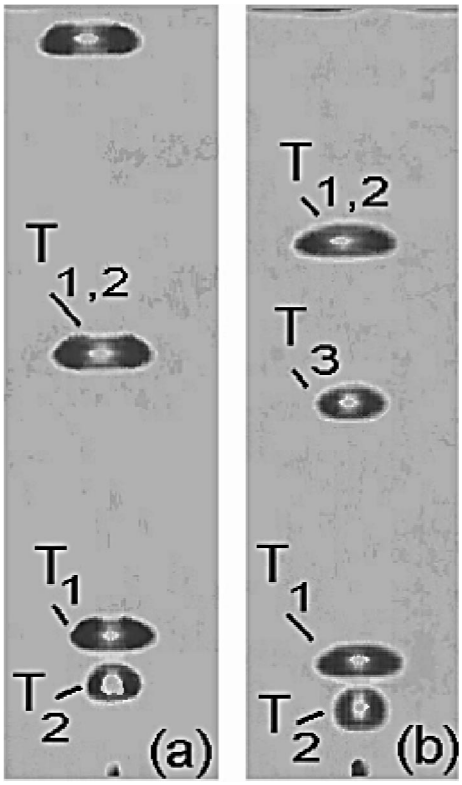

FIG. 12. Images of bistability. In (a) the bubbling is in period-2, in which these two bubbles (T_1 and T_2), close to the nozzle (represented by the lowest spot) will coalesce creating a large bubble similar to $T_{1,2}$. In (b) there is a period-3 bubbling regime, in which the two first bubbles coalesce forming a large bubble $T_{1,2}$ as in the previous case, but now there is a third noncoalescent bubble T_3 following the large bubble.

One notes that the greatest root model would become a smallest root model if $F_T(t)$ corresponded to a time dependent force balance during the formation of the bubble, with the function force F_T depending on the time T of the previous bubble. But the smallest root models did not reproduce the experimental diagrams as did the greatest root models.

This global understanding of the outcomes of this experiment allows us to concentrate efforts in the very mechanism of bubbling formation at fixed air flow rate and its connection with the parameters involved in the experimental apparatus, as for example the hose length.

ACKNOWLEDGMENT

This work was partially supported by the Brazilian agencies FAPESP and CNPq.

[1] G. Liger-Belair, Ann. Phys. (Paris) **27**, 1 (2002).
[2] R. Clift, J. R. Grace, and M. E. Weber, *Bubbles, Drops and Particles* (Academic, New York, 1978).
[3] Yu. A. Buyevich and B. W. Webbon, Chem. Eng. Sci. **51**, 4843 (1996).
[4] R. W. van den Berg, Ph.D. thesis, Delft University of Technology, 1996.
[5] V. S. M. Piassi, A. Tufaile, and J. C. Sartorelli, Chaos **14**, 477 (2004).
[6] A. Tufaile and J. C. Sartorelli, Physica A **275**, 336 (2000).
[7] D. J. Tritton and C. Egdell, Phys. Fluids A **5**, 503 (1993).
[8] L. J. Mittoni, M. P. Schwarz, and R. D. La Nauze, Phys. Fluids

7, 891 (1995).
[9] W. Ren, S. J. Hu, B. J. Zhang, F. Z. Wang, Y. F. Gong, and J. X. Xu, Int. J. Bifurcation Chaos Appl. Sci. Eng. **7**, 1867 (1997).
[10] A. V. Holden and Y. Fan, Chaos, Solitons Fractals **2**, 349 (1992).
[11] E. A. Jackson, *Perspectives of Nonlinear Dynamics* (Cambridge University Press, Cambridge, England, 1989).
[12] A. N. Pisarchik, R. Meucci, and F. T. Arecchi, Eur. Phys. J. D **13**, 385 (2001).
[13] A. B. Ponter and A. I. Surati, Chem. Eng. Technol. **20**, 85 (1997).
[14] K. Kaneko, Prog. Theor. Phys. **68**, 669 (1982).
[15] T. LoFaro, Math. Comput. Modell. **24**, 27 (1996).
[16] E. Yellin and A. Rabinovitch, Phys. Rev. E **67**, 016202 (2003).